

This paper has been approved for public release.
The clearance number is: 66ABW-2008-0112

Unmixing the Materials and Mechanics Contributions in Non-resolved Object Signatures

Anil Chaudhary, Craig Birkemeier
Applied Optimization, Inc., Dayton, OH 45402

Stephen Gregory, Tamara Payne
Boeing LTS, Kihei, HI 96753

James Brown
AFRL/RVBYB Hanscom AFB, MA 45433

ABSTRACT

Temporal behavior of a non-resolved resident space object [RSO] signature is a function of the abundance of its contributing materials. These abundances are, in turn, a function of the orbital behavior of the RSO. For example, in case of a spin-stabilized RSO, the abundances display a cyclic behavior. The present work uses a positive matrix factorization technique to extract the temporal variation of material abundances from hyperspectral or multi-spectral time-resolved signatures. A Fourier analysis of temporal variation of material abundance provides knowledge about the mechanics of the space object. This paper describes the unmixing and Fourier analysis process that, taken together, extract information about materials and mechanics from non-resolved RSO signatures. Unmixing results are presented for simulated hyperspectral signatures and for three- or four-color Johnson BVRI photometry observations data. These two situations cover the range of optics and sensor capabilities that may be available from a premier site for optical observations to a commercial-off-the-shelf small-aperture telescope site.

1. INTRODUCTION

Features in resident space object [RSO] signatures are a mixture of effects due to its range, solar illumination, material reflectance properties, and projected view of the RSO with respect to the sensor. Each component of this mixture can change with time. When one or more of these components are unknown, the signature can acquire a non-stationary or unsteady character; i.e. its temporal statistics change during observation. For example, for a stable RSO in geosynchronous orbit, its projected view would have a steady-state character for extended durations with respect to ground-based sensors. For space-based sensors, the viewing direction would change continuously. This blends with all other changes to increase complexity of the signature.

To learn about the behavior of an unknown RSO from its signature is a challenging task. Besides its range and solar phase angle, other components that influence its signature are unknown. Characterizing the unsteady nature of the signature by itself has limited benefits because no two RSO observations have identical conditions of illumination and RSO orientation, which means that the unsteady character of signature is also not the same from one observation to another. Thus it is important to search the signature for entities that are fundamentally related to the RSO in a way that their presence can be detected in a repeatable manner in multiple observations for the same RSO. In other words, signature analysis is deemed a process of unmixing, which seeks to isolate those entities that are 'invariant' during the time of observation. The present work considers two such entities. First is the set of materials that is persistent in the RSO signature. The second is the character of the projected view, which depends on the sensor position and the RSO stabilization scheme or lack/malfunction thereof. Or, for short, we term the first invariant entity as materials and the second entity as mechanics.

There is extensive literature on the use of unmixing techniques to identify terrestrial materials from remote sensing hyperspectral data collected by airborne and space-based sensors. Reference 1 provides a review of these methods. References 2-5 report on use of unmixing techniques for identification of materials in an

RSO signature. The terrestrial imaging from airborne sensors typically comprises extensive data sets and consequently its analysis and information extraction needs are extensive as well. The RSO signature data, however, is limited and thus there is a smaller choice in the techniques that may be used for unmixing. The work in References 2-5 analyzed RSO signature at a time instant. The data was collected using a spectrometer and it contained brightness values at approximately one hundred wavelengths in the visible spectrum. The frame rate for the instrument was not large enough to collect time resolved data. However, it is now anticipated that a new generation of sensors could have high enough data rate to collect time-resolved hyperspectral RSO signatures. This would be equivalent to collecting a hundred “light curves” simultaneously. Needless to say, there will be limitations on how faint the RSO may be. Nonetheless, the sensor developments make it attractive to extend and apply the unmixing methods to multi-spectral light curves in order to obtain a time history of material content of the RSO signature.

A first hypothesis of present work is that if one or more materials are persistently detected in multiple signature collections for the same RSO, then these materials are contained in the makeup of that RSO. To this end, the unmixing accuracy depends on the quality of the material spectra and signature data. The present work uses all available material spectra as input to unmixing and the algorithm chooses those spectra whose linear combination most closely reproduces the signature at a time slice. The calculation is repeated for the next time slice. As for the signature, accurate cancellation of atmosphere is a major consideration. This is particularly so for multi-spectral signatures in that the cancellation needs to account for the atmospheric effects that are a function of wavelength. With availability of sufficient resources, both the material spectra and signature related concerns could be addressed for a select set of RSOs and sensor sites. The resources, however, are almost always scarce. Thus this work assumes that there are imperfections in the material spectra and atmosphere cancellation and yet aims to extract a useful result.

Material spectra change with time due to aging in space. This change is a function of wavelength and is typically a few percent per year. Thus, for an older RSO, the accumulated effect due to aging can be significant. This extent of aging is known to vary from one RSO to another, even for those belonging to the same family. To account for aging, there are two options, neither of which is suited for this work because it assumes no prior knowledge of the RSO. [The first option is to use aging models and the second is to collect repeated observations over a long enough time scale.] Thus, this work uses all available spectra as input. If this input happens to include exact spectra for the materials present in the RSO signature, the unmixing error is minimized. However, this can rarely be the case. The unmixing algorithm needs to overcome this situation, at least in terms of quantifying the level of success attained in its results.

Output of unmixing is identification of materials and their respective contribution [albedo] in the RSO signature. The albedo values are normalized by the observed signature in order to compute abundance values. For example, if two materials are detected, the abundance values show that x-% of the signature is due to the first material, y-% is due to the second, and the balance of z %, where $z = (100 - x - y)$, could not be unmixed. The z % is measure of quality of unmixing and is used to establish unmixing error bounds on the results. A user may set a bound on the value of z in order to accept or reject the unmixing results.

A second hypothesis of the present work is that if the unmixing error bound is persistently below a threshold in multiple signature collections for the same RSO, then the time history of abundances for the persistently detected materials embeds knowledge of RSO mechanics. Consider a spin-stabilized RSO for example. If there are n-axes of symmetry, the abundance graph for one or more materials can contain a frequency as high as ($2n \times$ RSO rotational frequency), depending on how the projected view of the RSO changes with respect to the sensor during the observation period. In order to represent this frequency, the sampling rate for each band must be at least equal to ($2 \times 2n \times$ RSO rotational frequency). This is a challenge, particularly for a faint RSO, due to the integration time needed by the CCD.

Johnson BVRI photometry is a common mode for RSO signature data collection today. It is four-color data. Even though the future sensors will likely allow more bands, it is prudent to make use of available data to explore usefulness of the unmixing algorithm. Accordingly, this paper shows results obtained for two situations. The first set results are obtained by using simulated time-resolved hyperspectral signatures. The second set of results is obtained using actual Johnson BVRI observations data, which was collected

using a small aperture telescope. The former illustrates the potential of the unmixing method and latter puts in the context of practical considerations of today.

Consider an example where the RSO rotates once per minute, there is one axis of symmetry and the signature is to be collected in Johnson BVRI bands. Then the minimum required sampling rate is four times a minute [i.e., one four color observation every 15 seconds]. The present day practice is to use a filter wheel to collect data one band at a time. Thus, the available time observation in each band is < 4 seconds. This is inclusive of the integration time to collect the image on the CCD detector and the time it takes for the filter to switch from one band to next, which itself may be five seconds or larger. Most RSOs of interest are faint and the integration time can exceed five seconds as well. Thus, the data collected has an insufficient sampling rate for the case considered in this example. In such a case, the unmixing results are useful for identification of materials makeup of the RSO, but are insufficient for characterization of RSO mechanics.

Consider another example where the RSO is a three-axis stabilized satellite. It has a non-periodic signature, which could contain specular glints. Typically, a glint would result from a single material. For example, consider a case where the solar phase-angle bisector matches with the normal to the solar panel. Then, the observed signature will contain a glint [Reference 6]. It is unlikely that this phase angle bisector condition will be reached for other RSO surfaces at the same time. Thus a larger portion of the signature will be the solar panel albedo. Also, when such a glint is incipient, the rate of change of albedo for the solar panel will be much larger than that for other materials. This difference can be used to differentiate a specular glint from RSO mechanics.

In the following, Section 2 describes the unmixing algorithm, Section 3 shows the results obtained for simulated hyperspectral data, Section 4 shows the results for Johnson BVRI photometry data, Section 5 lists the conclusions, and Section 6 contains acknowledgements.

2. UNMIXING ALGORITHM

This work makes three contributions to unmixing. First it shows that unmixing can be used to isolate materials and mechanics in the RSO signature and shows a metric for quality of results that are obtained using available material spectra. Second is that its application is not limited to hyperspectral data. It can be used with signatures containing three- or four-color data. This makes it useful not only for the sensors of tomorrow, but also for the data that can be collected today using small aperture telescopes. The third is that it is developed for time resolved signatures instead of a single time slice of data, which shows how the albedo and abundance of each material is changing.

The percentage of light contributed by a material to the RSO signature must always be positive. This is enforced in the numerical solution using the positive matrix factorization technique described in Reference 7. It uses a simple transformation to ensure that albedo is always positive. It expresses albedo of each material as being equal to $\exp(\alpha)$ and then the numerical solution solves for the value of α . Irrespective of whether α is positive or negative, the albedo is always positive. This allows the numerical solution to be performed with no constraints and allows for a quicker solution. There are multiple means to find the albedo contributions as reported in References 2-5, and any of the methods can be used. The work uses minimization of weighted residuals, nonlinear least squares and singular value decomposition techniques.

The unmixing calculation begins with a set of common spacecraft/debris material spectra and an RSO signature as input. Let the signature contain n -bands and let there be m -material spectra [$m \geq 3$]. Typically n is less than m , which results in a rectangular system of equations. The algorithm begins by assuming that each of the m -materials is equally likely to be present in the signature. It then determines the weights for each of the m -spectra such that the resulting albedo represents the observed signature at each time instant with maximal accuracy. A time history of the albedo contributions is obtained by concatenating the results at each time slice. The materials that contribute more than 5% to the signature at more than 75% of the time instants are retained. Typically, the retained albedo contributions cannot account for all of the spectral content in the signature. This unaccounted spectral content is identified as unmixing error. It is assumed that the error in each spectral band is uncorrelated and is normally distributed. This is used to compute the

median and standard deviation of the error, which are then used to estimate an unmixing error bound. Unmixing solution is rejected at any time slice where the error bound exceeds 20%.

Proving lack of bias in an unmixing solution is difficult when the exact material spectra are unknown. The present work uses all available material spectra as input with the intent that a true material spectrum could be represented as a linear combination thereof. However, this is not guaranteed. In cases when > 80% of the spectral content of a RSO signature is consistently accounted for by the same material spectra in multiple observations, it is unlikely that the identified materials are incorrect. This could be attributed to two reasons. First, each collection of RSO signature is an independent event. Second, a time resolved signature typically contains multiple time instances where the signature spectral components are linearly independent. It is unlikely that a same incorrect conclusion can be reached in multiple independent events.

Unmixing provides an additive decomposition of the RSO signature into percent contributions. Each contribution is a unit-less number. The signature data, however, is in visual magnitude. Thus, prior to unmixing, the signature is converted to a non-dimensional form in two steps. First, the visual magnitude value of brightness in each band is converted to flux units and is normalized with the solar irradiance value at that wavelength. Since a sensor could be either space-based or ground-based, the solar irradiance value used is for the top of the atmosphere or at sea level, respectively. This non-dimensional signature is unmixed using a set of common spacecraft/debris material spectra [see Figure 2.1]

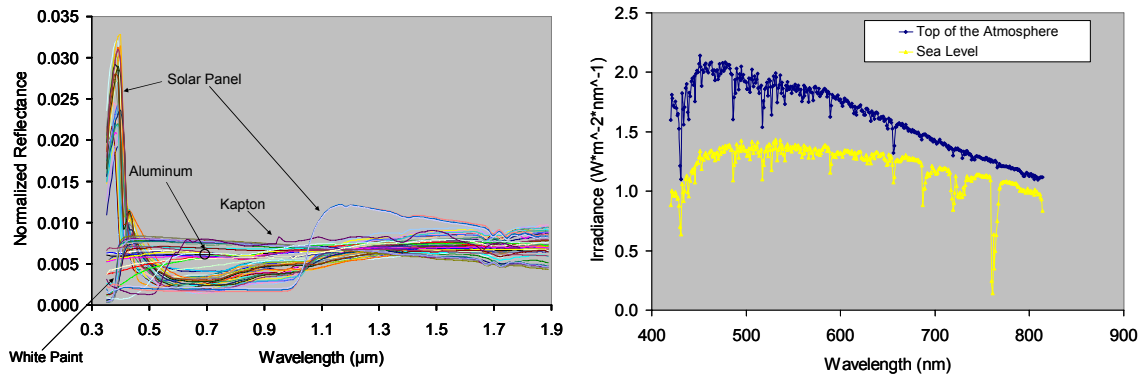


Figure 2.1: Common Spacecraft/Debris Material Spectra [from References 8-10] and the Solar Radiation Spectrum at the Top of the Atmosphere and at Sea Level

3. UNMIXING OF SIMULATED HYPERSPECTRAL DATA

The purpose of examples and results in this section is to show that unmixing can identify correct materials from simulated signature data and can express the RSO mechanics information embedded in the signature in terms of temporal plots of material abundance. The results have been obtained in two steps. First, a notional observation scenario is considered for a stable or unstable RSO [see Figure 3.1], which is being observed by a space-based hyperspectral sensor. The simulated signature is generated by choosing one solar panel and one aluminum spectrum from Figure 2.1. In all cases, the solar phase angle, direction of illumination for each of the RSO surfaces, and its projected view including any self occultations are continuously changing with respect to the space based sensor. These calculations were performed using the POSE software [Reference 11-12]. Second, it is presumed that the signature is for an unknown RSO and is unmixed by using all available material spectra in Figure 2.1. The algorithm is found to correctly identify the material spectra that were used in the generation of signature in the first step and shows the time evolution of abundance for each material.



Figure 3.1: Notional RSO whose makeup comprises two Materials: Solar Panel and Aluminum

Notional Three-axis stabilized Satellite: This considers the RSO in Figure 3.1 to be three-axis stabilized object. Figure 3.2a shows the simulated signature and Figure 3.2b shows the time evolution of abundance for solar panel and aluminum. The abundance values change little over the duration of observation, which is consistent with a stable RSO.

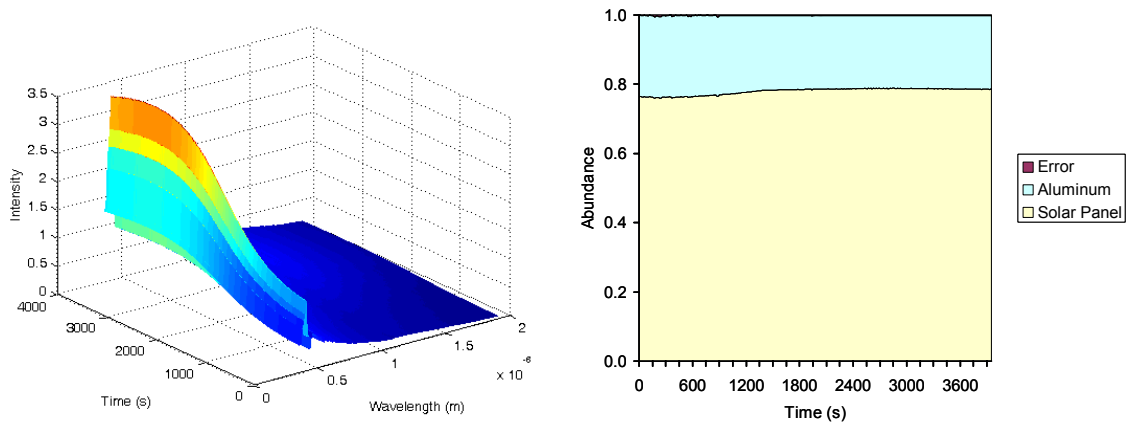


Figure 3.2: Simulated Signature and Time Evolution of Abundance for the Two Materials

Notional Single-axis Tumble: This considers the RSO in Figure 3.1 to be tumbling about its orbit normal axis. The tumble frequency was 0.0167 Hz, or once every minute. Figure 3.3a shows the simulated signature, and Figure 3.3b shows the time evolution of abundances and the unmixing error. The solar panel contribution is shaded light yellow, the aluminum contribution is shaded light blue and the unmixing error is shown in orange. The two abundances and the unmixing error add to 100%. The evolution of material abundance is a mixture of two behaviors. First is the RSO tumble, and second is the movement of the space-based sensor itself. Fourier analysis of the abundance graph shows a prominent frequency of 0.0167 Hz, which is the tumble frequency.

Notional Three-axis Tumble: This considers the RSO in Figure 3.1 to be unstable and tumbling along three axes. The three-axis tumble was purposefully chosen such that the rotational frequencies of the RSO are changing quickly. The generation of the signature was performed in two steps. First the RSO principal rotational inertia tensor was computed, and its three-axis tumble behavior was simulated using the Euler equations for torque free tumble. Figure 3.4 shows the time evolution of RSO rotational frequencies predicted by the Euler equations. The frequencies, themselves, are changing. This simulation also generated the temporal evolution of RSO orientation, which is a function of the rates of rotation along each of the three axes of tumble. In the second step, the RSO orientation information was input to the POSE software for generation of illumination conditions and projected view with respect to a space-based sensor. Figure 3.5a shows the simulated signature and Figure 3.5b shows the abundance graph for the solar panel and aluminum, and also that for the unmixing error. A Fourier analysis of the abundance shows frequencies up to 0.035 Hz, which is about twice the rate of tumble. This result shows that a complex signature can be condensed into a one-dimensional graph of abundance that embodies the RSO mechanics information.

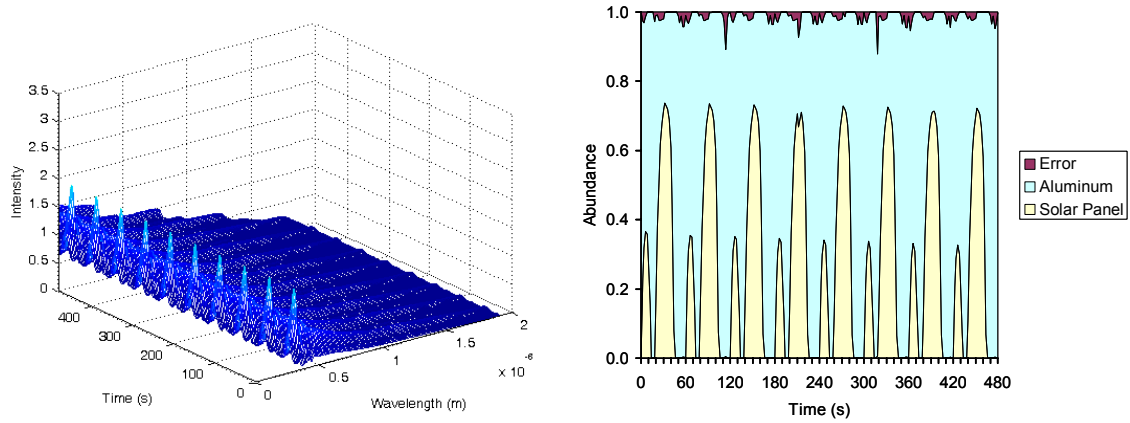


Figure 3.3: Simulated Signature and Time Evolution of Abundance for the Two Materials

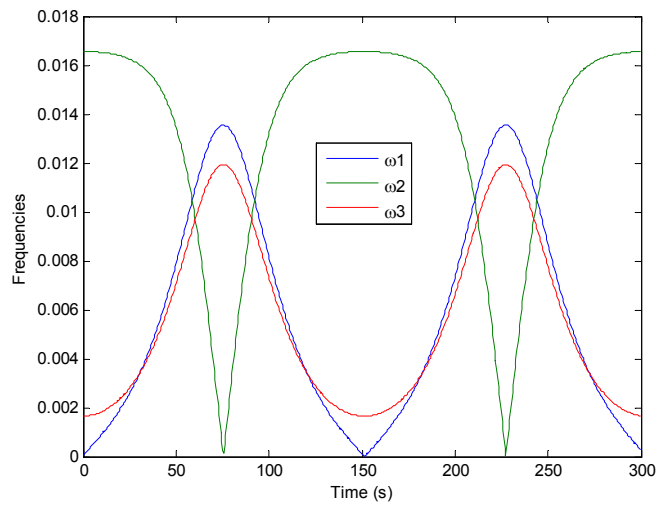


Figure 3.4: Time Evolution of Frequencies in Three-Axis Tumble of an RSO

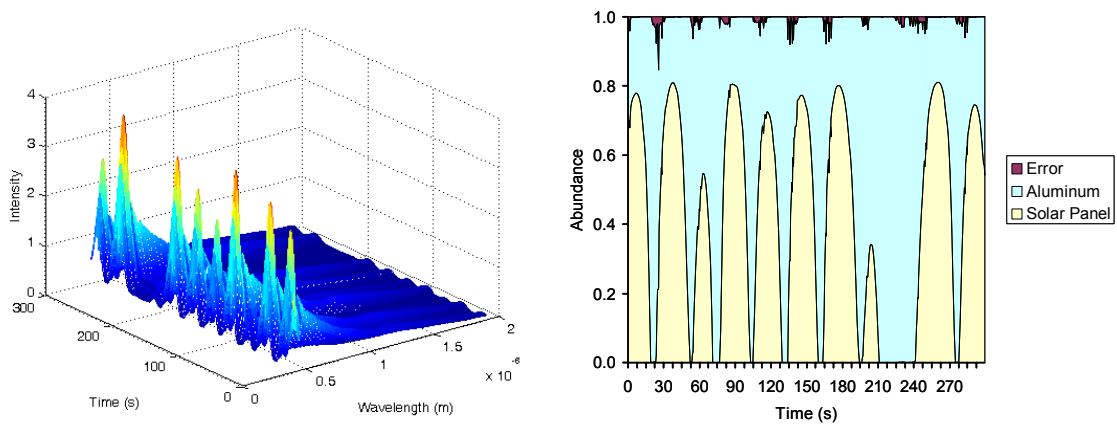


Figure 3.5: Simulated Signature and Time Evolution of Abundance for the Two Materials

4. UNMIXING OF JOHNSON BVRI PHOTOMETRY OBSERVATIONS DATA

In this section, results are presented for material makeup of eight different RSOs. The results are obtained by unmixing three- or four-color data in the Johnson BVRI photometry observations, which were collected using a ground-based, commercial-off-the-shelf 16" diameter telescope. The signature is collected one color at a time. Thus, each spectral component of signature is actually the satellite signature in that band at a different time instant. The time required to collect a single observation is roughly 5-10 seconds, with approximately 2 seconds of 'dead time' between observations [resulting from both readout time and turning of the filter wheel]. Each set of three- or four-color data is available every eight minutes. The unmixing results are given in the following for the median and standard deviation values for the abundances.

The signatures considered are for RSOs that belong to two different families, which are denoted as A and B, respectively. There are two members of A and there are six members of B. Figure 4.1 show signatures for RSOs A-1 and A-2 [References 10 and 13]. Figure 4.2 shows signatures for RSOs B-1 to B-6 [References 10 and 13]. Figure 4.3 shows a tabular summary of the median values of the material abundance values obtained by unmixing. The material makeup shown in Figure 4.3 includes only those materials that were detected in > 75% of the data points in each signature and when the unmixing error bound is < 20%. Each unmixing calculation was performed using the material spectra shown in Figure 2.1. All RSOs showed presence of solar panel and aluminum.

The results are consistent in the detection of materials and their abundance values. Although the unmixing error was small, the standard deviation was larger for the three-band data as compared to the four-band data. The three-band data also contained specular glints, where the relative brightness of the spectral components changes significantly and the abundance values showed a larger scatter, which was manifested in the higher values of standard deviation. Although this effect will become smaller if the signature contains more colors, it is valuable to explore enhancements to the algorithm so that it can be used with data that is easier and/or less expensive to acquire.

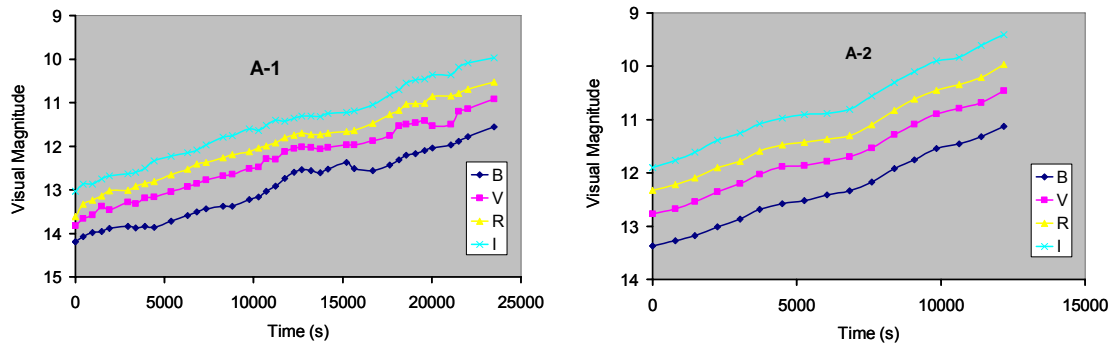


Figure 4.1: Johnson BVRI Signatures for RSO A-1 and A-2

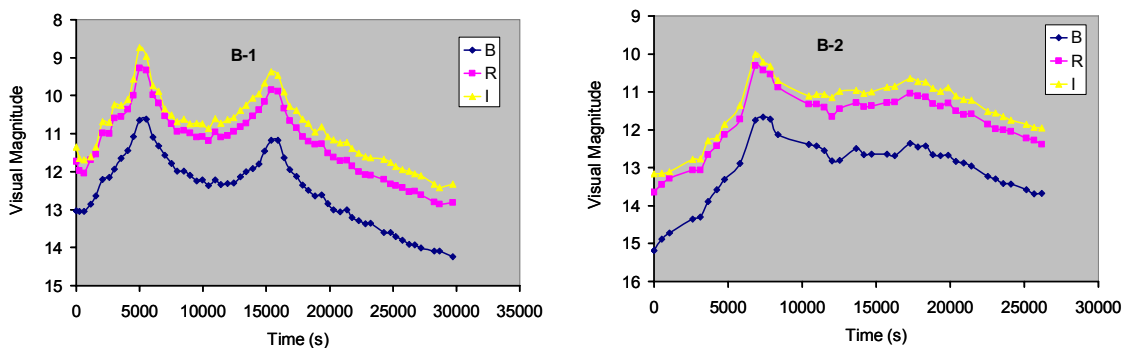


Figure 4.2a: Johnson BVRI Signatures for RSO B-1 and B-2

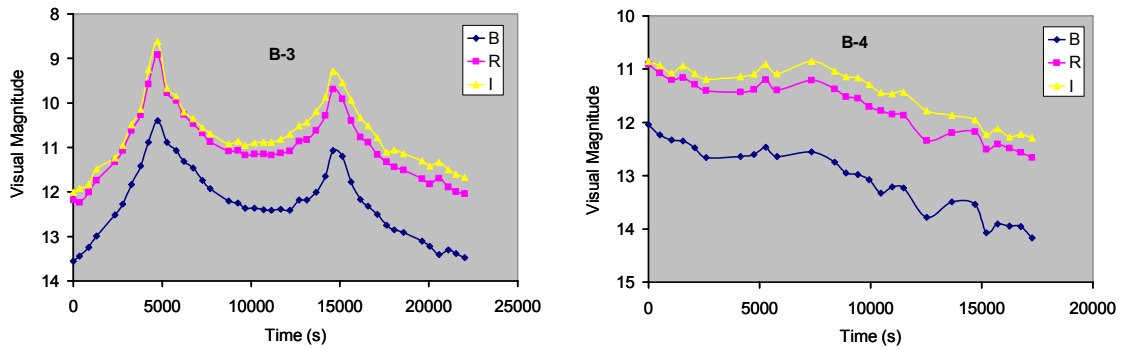


Figure 4.2b: Johnson BVRI Signatures for RSO B-3 and B-4

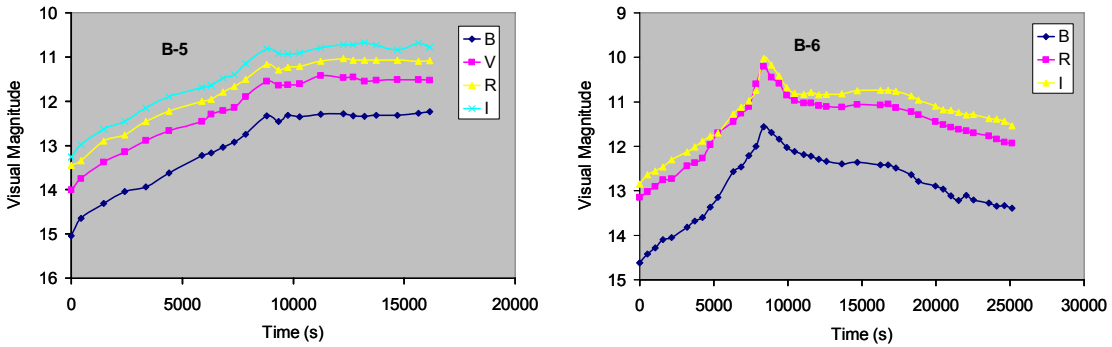


Figure 4.2c: Johnson BVRI Signatures for RSO B-5 and B-6

RSO	% Solar Panel	% Aluminum
A-1	60 [$\sigma = 9$]	35 [$\sigma = 7$]
A-2	70 [$\sigma = 3$]	23 [$\sigma = 1$]
B-1	37 [$\sigma = 12$]	59 [$\sigma = 12$]
B-2	37 [$\sigma = 9$]	60 [$\sigma = 10$]
B-3	41 [$\sigma = 14$]	57 [$\sigma = 16$]
B-4	35 [$\sigma = 16$]	63 [$\sigma = 14$]
B-5	49 [$\sigma = 6$]	45 [$\sigma = 6$]
B-6	40 [$\sigma = 12$]	52 [$\sigma = 14$]

Figure 4.3: Median and Standard Deviation of Material Abundance Values

5. CONCLUSIONS

This paper presents two hypotheses for determination of material makeup and RSO mechanics on the basis of unmixing multi-color RSO signatures. The unmixing error bound is used as a measure of quality of the unmixing results. Simulated hyperspectral signatures and three- or four-color Johnson BVRI signatures data were unmixed in order to substantiate the two hypotheses. It is shown that signature unmixing provides consistent and usable results for material makeup of RSOs.

The results for hyperspectral time-resolved signatures show how unmixing can extract knowledge of RSO mechanics and materials using a sensor that could be located at a premier site for optical observations such as the Air Force Maui Optical Station. The results for three- or four-color signatures show how the same technique can extract knowledge of RSO materials by making use of an inexpensive commercial-off-the-

shelf [COTS] telescope. Ability to extract information about mechanics is limited by the frame rate that is feasible with COTS telescopes. Between these two bounds of capabilities of optics and detector equipment, there are numerous combinations and trade-offs feasible at different observation sites. For each of these situations, the benefits of unmixing a color signature will lie within the bounds of being able to understand both the RSO materials and mechanics to being able only identify the materials and their median contribution to the signature. Furthermore, the time to unmix a signature using a desktop PC is in seconds, and thus the additional knowledge that can be obtained from unmixing comes at practically no cost.

6. ACKNOWLEDGEMENT

This work is supported by an AFRL/Space Vehicle SBIR Phase II project [Contract No: FA8718-07-C-0024]. The progress in this work is built upon the developments performed in an ongoing AFRL/Sensors Directorate SBIR Phase III effort [Contract No: FA8650-05-D-1858]. We are thankful to Kira Abercromby [NASA Johnson Space Center] and Kris Hamada [Boeing LTS] for providing the material spectra.

7. REFERENCES

1. Keshava, N., "A Survey of Spectral Unmixing Algorithms", MIT Lincoln Laboratory Journal, Vol. 14, No.1, 2003
2. Jorgensen, K., Africano, J., Hamada, K., Stansbury, E., Sydney, P., and Kervin, P., "Physical Properties of Orbital Debris from Spectroscopic Observations", *Advances in Space Research* 34 (2004) 1021-1025.
3. Hamada, K., "Spectral Unmixing Methods for Non-Resolved Space Object Characterization", AMOS Technical Conference 2005.
4. Brevdo, E., Luu, K.K., "Improving the Hyperspectral Linear Unmixing Problem with Unsupervised Cluster and Covariance Estimates", in *Algorithms and Technologies for Multispectral, Hyperspectral, and Ultraspectral Imagery XII*, edited by Shen, S.S., Lewis, P.E., Proc. of SPIE Vol. 6233.
5. Matson, C.L., Giffin, S.M., Hamada, K., Lambert, J., Luu, K., "The Effects of Class Size and Separation on Fractional Abundance Estimates", AMOS Photometry Workshop, March 2004.
6. Lambert, J., "Optical Glint Analysis Techniques", in AMOS Photometry Workshop 2006 on Space Surveillance Using Passive Optical Techniques for Non-Resolvable Space Object Identification
7. Kaasalainen, M., Torppa, J., "Optimization Methods for Asteroid Lightcurve Inversion. Part I: Shape Determination and Part II: The Complete Inverse Problem", in *ICARUS* 153, pp 24-51, 2001.
8. Abercromby, K., personal communication, 2007.
9. Hamada, K., personal communication, 2007.
10. Gregory, S., personal communication, 2008.
11. Chaudhary, A., Birkemeier, C., Wilhelm, S., "PANOPTES: Photometry Analysis Optical Tracking and Evaluation System," AFRL-SN-WP-TR-2007-1222, January 2008, pp. 18.
12. Chaudhary, A., Stewart, J., Klem, B., "Near-Real Time Utilization of Multicolor Nonresolved Signature for Satellite Characterization," AFRL-SN-WP-TR-2005-1119, May 2005.
13. Payne, T., "Statistical Properties of Geosynchronous Satellite Photometric Signatures", in AMOS Photometry Workshop 2006 on Space Surveillance Using Passive Optical Techniques for Non-Resolvable Space Object Identification.